Retaining Wall with Reinforced Cohesionless Backfill

By Swami Saran,[1] K. G. Garg,[2] and R. K. Bhandari[3]

Abstract: The case of a rigid wall retaining a reinforced cohesionless fill that carries a uniform surcharge load has been analyzed based on the limit equilibrium approach. The reinforcement may be in the form of strips or mats that are not connected to the wall. This analysis considers the stability of an element of the failure wedge, which is assumed to develop in the reinforced earth mass adjoining the back face of the wall. Nondimensional design charts have been developed for computing the resulting lateral earth pressure on the wall and the height of its point of application above the base of the wall. The theoretical findings have been verified in two different sets of model tests on a rigid wall that is retaining a dry sand fill and that is reinforced by aluminium and bamboo strips. Experimental results are in good agreement with the theoretical predictions. An applied example for an 8-m high wall illustrates the design procedure.

Introduction

Reinforced earth wall construction is becoming popular in many countries. In this type of construction, the reinforcing strips are connected to the wall [Fig. 1(*a*)]. The lateral thrust on the wall is almost eliminated due to the development of soil–reinforcement interface friction and bearing. Therefore, a thin wall element known as skin is found adequate to retain the backfill resulting in considerable economic savings. However, in India, the technique has not yet found acceptance due to limited awareness of the approach among practicing engineers, as well as the high cost of reinforcing materials. An alternative technique is a rigid wall in which the backfill is reinforced with strips not tied to the wall [Fig. 1(*b*)]. This technique is considered appropriate and acceptable to Indian conditions. In this type of construction, the earth pressure on the wall is reduced significantly. Further, there are economic benefits due to the elimination of fixtures, the use of cheaper reinforcing materials such as bamboo strips, and a reduction in the level of skilled labor required.

Some studies on the performance of rigid walls with reinforced backfill (i.e., reinforcing strips not attached to the wall) are reported in the literature. On the basis of model test results, Hausmann and Lee (1978) reported about a 40% reduction in the moment at the base of the wall by reinforcing the dry cohesionless backfill soil. Nondimensional design curves were provided by Talwar (1981) for computing the resulting lateral earth pressure and the height of its point of application above the base of a rigid wall retaining a reinforced cohesionless fill.

These studies illustrate the effectiveness of unattached reinforcement in reducing the lateral earth pressure on a rigid wall. However, the effect of

[1]Prof., Civ. Engrg. Dept., Univ. of Roorkee, Roorkee 247 667, India.
[2]Sci., Central Bldg. Res. Inst., Roorkee 247 667, India.
[3]Chf. Tech. and Sr. Engrg. Advisor, UNCH (Habitat) NBRO, Colombo, Sri Lanka.

Note. Discussion open until May 1, 1993. To extend the closing date one month, a written request must be filed with the ASCE Manager of Journals. The manuscript for this paper was submitted for review and possible publication on February 2, 1990. This paper is part of the *Journal of Geotechnical Engineering*, Vol. 118, No. 12, December, 1992. ©ASCE, ISSN 0733-9410/92/0012-1869/$1.00 + $.15 per page. Paper No. 27000.

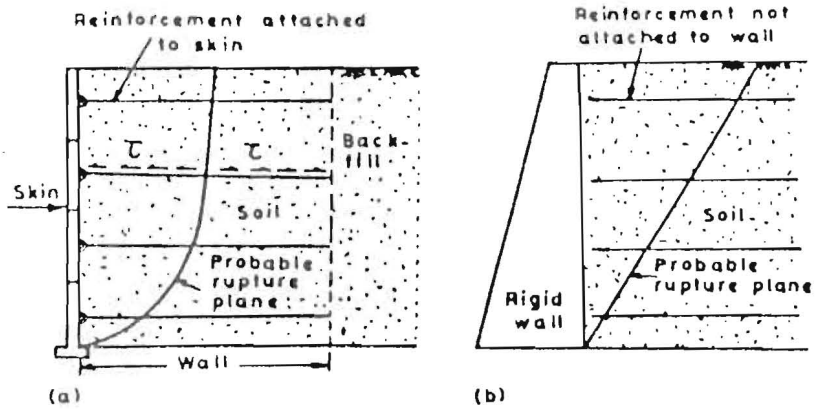

FIG. 1. Sections: (*a*) Reinforced Earth Wall; (*b*) Rigid Wall with Reinforced Backfill

external loading on the surface of the backfilled earth was not considered in these studies. In practice, the backfill often must support external loadings. Thus, there is a need to develop an analysis for the design of rigid walls that retain reinforced fill while supporting external loading on their surfaces. An attempt has been made to develop an analysis applicable to both strip and mat-type reinforcements.

Theoretical Analysis

The following assumptions were made in order to proceed with the analysis of a rigid wall retaining reinforced fill:

1. The backfill is homogeneous, isotropic, and cohesionless.
2. The coefficient of friction between the soil and the reinforcement is independent of the overburden pressure and the dimensions of the reinforcement.
3. The failure surface is a plane passing through the heel of the retaining wall.
4. The frictional resistance offered by each reinforcing strip to the lateral movement of the wedge is uniformly distributed over a fill height equal to the vertical spacing of the reinforcement encompassing that fill layer.
5. Only the part of the strip that experiences movement of soil, relative to itself, will be assumed to be contributing frictional resistance.
6. The retaining wall rotates about its base and away from the fill sufficiently to cause mobilization of full soil-strip frictional resistance.
7. No water pressures develop within the reinforced backfill.

This analysis is for a retaining wall of height H with a vertical back face. The wall retains a cohesionless backfill that has a dry density γ and an angle of internal friction ϕ. The backfill carries a uniform surcharge of intensity q. The backfill is reinforced with unattached horizontal strips of length L and width w, placed at a vertical spacing of S_v and a horizontal spacing of S_h. A failure plane BC, making an angle θ with the vertical, passes through the heel of the retaining wall (Fig. 2).

The frictional resistance offered by a reinforcing strip will be located in the shorter portion of the strip, which moves relative to the failure plane. The shorter portion of the strip is referred as the effective length. For example, if strip DF is cut by failure plane at E, then the effective length

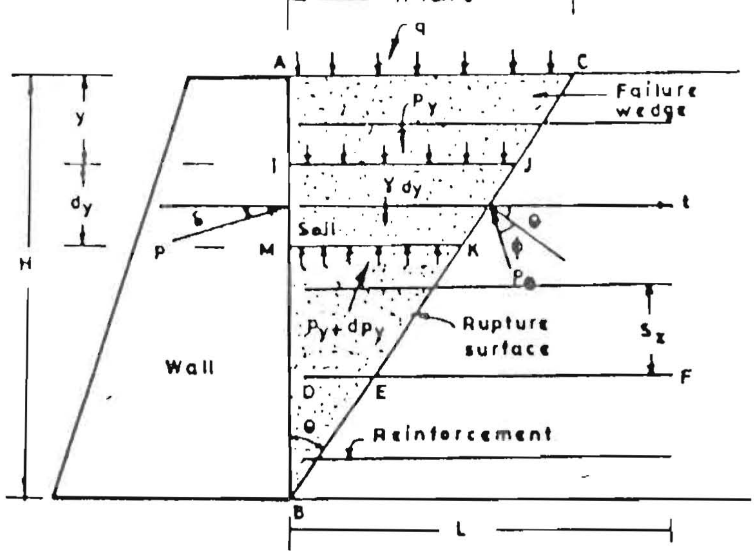

FIG. 2. Failure Wedge and Various Intensities of Forces Keeping Element IJKM in Equilibrium

will be either DE or EF. In the case in which the portion of the strip length within the wedge DE < EF, then EF will not move out of the soil mass. DE will come out of the wedge as the latter moves away from the stationary portion of the backfill. If EF < DE, the strip will move with the failure wedge, pulling length EF out of the stationary mass of backfill. Therefore, the effective length of the strip will be the smaller of DE or EF. A reinforcing strip, located completely within the moving wedge, will not contribute any frictional resistance to the movement of the wedge.

An element IJKM (Fig. 2) of the failure wedge of thickness dy, located at a distance y from the top of the wedge, is in equilibrium under the following intensities of forces: p_y = pressure intensity acting uniformly on IJ in the vertical direction due to the self-weight of the backfill lying above IJ and to the uniform surcharge q; $(P_y + dp_y)$ = uniform reaction intensity acting upward on KM in the vertical direction; p_θ = reaction-intensity on JK acting at an angle ϕ to the normal on JK; p = pressure-intensity on IM acting at an angle δ to the normal on IM; σ_n = vertical stress due to the weight of an element IJKM acting downward, or

$$\sigma_n = \gamma \cdot dy \qquad (1)$$

and $t = (T/S_z)$ = intensity of tension in the reinforcing strip, which is assumed to be transmitted uniformly to the soil layers of thickness S_z encompassing the strip.

Neglecting second-order and higher order terms, the static equilibrium of an element IJKM ($\Sigma H = 0$, $\Sigma V = 0$, and $\Sigma M = 0$) of failure wedge ABC (Fig. 2) yields the following relationships:

$$p_\theta = \frac{p \cos \delta + t}{\cos(\theta + \phi)\sec \theta} \qquad (2)$$

$$\frac{dp_y}{dy} = \frac{p_y + \gamma(H - y)}{H - y} - \frac{p \sin \delta}{(H - y)\tan \theta} - \frac{p_\theta \sec \theta \sin(\theta + \phi)}{(H - y)\tan \theta} \qquad (3)$$

$$\frac{dp_v}{dy} = \gamma - \frac{2p \sin \delta}{(H - y)\tan \theta} \quad \ldots\ldots (4)$$

All notations used are explained as shown in Fig. 2. Substituting p_0 from (2) into (3), equating it with (4), and solving for p, we get

$$p = \frac{p_v \tan \theta}{\cos \delta \tan(\theta + \phi) - \sin \delta} - \frac{t \tan(\theta + \phi)}{\cos \delta \tan(\theta + \phi) - \sin \delta} \quad \ldots\ldots (5)$$

On differentiating (5), substituting for (dp_v/dy) from (4), and using trigonometric identities

$$\frac{dp}{dy} = -C_1 \frac{p}{H - y} + C_2\gamma - C_3 \frac{dt}{dy} \quad \ldots\ldots (6)$$

where

$$C_1 = \frac{2 \sin \delta \cos(\theta + \phi)}{\sin(\theta + \phi - \delta)}$$

$$C_2 = \frac{\tan \theta \cos(\theta + \phi)}{\sin(\theta + \phi - \delta)}$$

$$C_3 = \frac{\sin(\theta + \phi)}{\sin(\theta + \phi - \delta)} \quad \ldots\ldots (7)$$

Tension T at the limiting equilibrium can be taken as

$$T = \frac{2wf^*\sigma_v l'}{S_x} \quad \ldots\ldots (8a)$$

where l' = effective length of strip, and

$$\sigma_v = \left(y + \frac{dy}{2}\right)\gamma + q \quad \ldots\ldots (8b)$$

where q = uniformly distributed external loading on the surface of the retained soil. l' will vary for each reinforcing strip, depending on the wedge angle θ and the length L of the strip as shown in Fig. 3.

1. Case 1: $H \tan \theta \leq (L/2)$

$$l' = (H - y)\tan \theta \quad \ldots\ldots (9)$$

2. Case 2: $(L/2) \leq H \tan \theta \leq L$

$$(H - Z_1)\tan \theta = \frac{L}{2} \quad \ldots\ldots (10a)$$

or

$$Z_1 = H - \frac{L}{2} \cot \theta \quad \ldots\ldots (10b)$$

$$l' = L - (H - y)\tan \theta, \qquad \text{for } y \leq Z_1 \quad \ldots\ldots (10c)$$

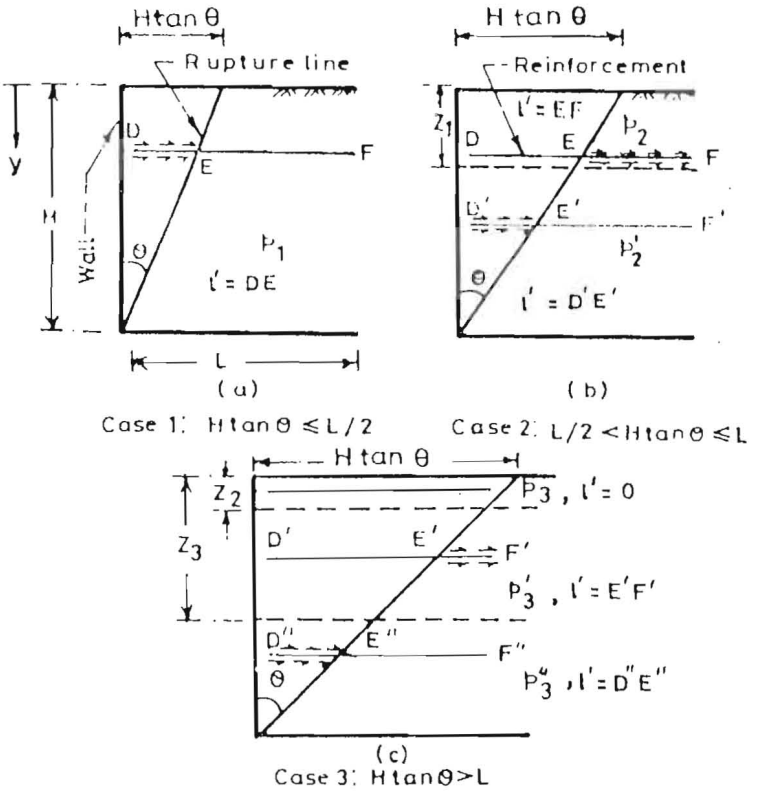

FIG. 3. Effective Length Criteria of Reinforcing Element

$$l' = (H - y)\tan\theta, \qquad \text{for } y > Z_1 \quad \ldots\ldots (11)$$

3. Case 3: $H \tan\theta \geq L$

$$(H - Z_2)\tan\theta = L \quad \ldots\ldots (12a)$$

or

$$Z_2 = H - L\cot\theta \quad \ldots\ldots (12b)$$

and

$$(H - Z_3)\tan\theta = \frac{L}{2} \quad \ldots\ldots (12c)$$

or

$$Z_3 = H - \frac{L}{2}\cot\theta \quad \ldots\ldots (12d)$$

therefore $Z_3 = Z_1$

$$l' = 0, \qquad \text{for } y \leq Z_2 \quad \ldots\ldots (13)$$

$$l' = L - (H - y)\tan\theta, \qquad \text{for } Z_2 \leq y \leq Z_3 \quad \ldots\ldots (14)$$

$$l' = (H - y)\tan\theta, \qquad \text{for } y > Z_3 \quad \ldots\ldots (15)$$

Z_1, Z_2, and Z_3 are shown in Fig. 3.

Differential equation (6) is solved for these three cases separately. Boundary conditions for the three cases are as follows:

1. Case I: $H \tan \theta \leq L/2$; [see Fig. 3(*a*)]

$$p_y = q, \quad \text{at } y = 0 \quad \ldots\ldots (16)$$

Pressure intensity p in this case is represented by p_1.

2. Case II: $L/2 < H \tan \theta \leq L$; [see Fig. 3(*b*)]. Pressure intensities in this case are represented by p_2 and p_2' in zone Z_1 and $H - Z_1$, respectively.

3. Case III: $H \tan \theta > L$; [see Fig. 3(*c*)]. Pressure intensities in this case are represented by p_3, p_3', and p_3'' in zones Z_2, $Z_3 - Z_2$, and $H - Z_3$, respectively.

The procedure for deriving expressions for pressure intensity, resultant earth pressure, and the height of the point of application of the resultant earth pressure above the base of the wall is discussed for case I only. Similar procedures have been adopted for cases II and III.

In case I, tension stress t is

$$t = \frac{2wf^*(H - y)\tan \theta \left[\gamma \left(\frac{y + dy}{2}\right) + q\right]}{S_x S_z} \quad \ldots\ldots (17)$$

Differentiating (17) and omitting small quantities of second order gives

$$\frac{dt}{dy} = \frac{2wf^* \tan \theta}{S_x S_z} [(H - 2y)\gamma \pm q] \quad \ldots\ldots (18)$$

$$\frac{dt}{dy} = K \left[\frac{(H - 2y) - q}{\gamma}\right] \quad \ldots\ldots (19)$$

where

$$K = \frac{2wf^*\gamma \tan \theta}{S_x S_z} = D_p \cdot \frac{2\gamma \tan \theta}{H} \quad \ldots\ldots (20a)$$

where

$$D_p = \frac{f^* wH}{S_x S_z} \quad \ldots\ldots (20b)$$

It may be noted that D_p is a nondimensional coefficient. For a given height of wall H and reinforcing material (f^* and w), D_p is controlled by the horizontal and vertical spacings of the reinforcement and is termed the spacing coefficient. Eq. (6) now becomes

$$\frac{dp}{dy} = -C_1 \frac{p}{(H - y)} + C_2\gamma - C_3 k \left[(H - 2y) - \frac{q}{\gamma}\right] \quad \ldots\ldots (21)$$

Substituting C_4 for $C_3 K$

$$\frac{dp}{dy} = -C_1 \frac{p}{H - y} + C_2\gamma - C_4 \left[(H - 2y) - \frac{q}{\gamma}\right] \quad \ldots\ldots (22)$$

The differential equation (22) is solved for the relevant boundary condition, i.e., $p_y = q$ at $y = 0$, and yields the following solution:

$$p_1 = -\left[\left(1 - \frac{y}{H}\right) - \left(1 - \frac{y}{H}\right)^{C_1}\right]\left[\frac{C_2\gamma H}{(1 - C_1)} + \frac{C_4 H^2}{(1 - C_1)}\right]$$

$$+ \left[\left(1 - \frac{y}{H}\right)^2 - \left(1 - \frac{y}{H}\right)^{C_1}\right]\frac{2C_4H^2}{(2 - C_1)} - \frac{C_4 Hq}{\gamma(1 - C_1)}\left[\left(1 - \frac{y}{H}\right)\right.$$

$$\left. - \left(1 - \frac{y}{H}\right)^{C_1}\right] + \left(1 - \frac{y}{H}\right)^{C_1}\left[\frac{q \tan\theta - t_{qo}\tan(\theta + \phi)}{\cos\delta \tan(\theta + \phi) - \sin\delta}\right] \quad \ldots\ldots (23)$$

where

$$t_{qo} = \frac{2wf^* Hq \tan\theta}{S_x S_z} \quad \ldots\ldots (24)$$

For presenting the results in nondimensional form, lateral earth pressure p_1 is considered to consist of the following two parts: (1) Lateral earth pressure due to backfill earth $p_{1\gamma}$; and (2) lateral earth pressure due to surcharge load p_{1q}; i.e.

$$p_1 = p_{1\gamma} + p_{1q} \quad \ldots\ldots (25)$$

where

$$p_{1\gamma} = -\left[\left(1 - \frac{y}{H}\right) - \left(1 - \frac{y}{H}\right)^{C_1}\right]\left[\frac{C_2\gamma H}{(1 - C_1)} + \frac{C_4 H^2}{(1 - C_1)}\right]$$

$$+ \left[\left(1 - \frac{y}{H}\right)^2 - \left(1 - \frac{y}{H}\right)^{C_1}\right]\frac{2C_4H^2}{(2 - C_1)} \quad \ldots\ldots (26)$$

and

$$p_{1q} = \frac{C_4 Hq}{\gamma(1 - C_1)}\left[\left(1 - \frac{y}{H}\right)^{C_1} - \left(1 - \frac{y}{H}\right)\right] + \left(1 - \frac{y}{H}\right)^{C_1}$$

$$\cdot \left[\frac{q \tan\theta - t_{qo}\tan(\theta + \phi)}{\cos\delta \tan(\theta + \phi) - \sin\delta}\right] \quad \ldots\ldots (27)$$

Expressions for pressure intensities $p_{2\gamma}$, $p'_{2\gamma}$, p_{2q}, and p'_{2q} [Fig. 3(*b*)] for case 2 and $p_{3\gamma}$, $p'_{3\gamma}$, $p''_{3\gamma}$, p_{3q}, p'_{3q}, p''_{3q} [Fig. 3(c)] for case 3 were obtained by the same approach (Garg 1988).

The nondimensional expressions for pressure intensities were obtained by dividing the terms $p_{1\gamma}$, $p_{2\gamma}$, $p'_{2\gamma}$, $p_{3\gamma}$, $p'_{3\gamma}$, and $p''_{3\gamma}$ by γH and p_{1q}, p_{2q}, p'_{2q}, p_{3q}, p'_{3q}, and p''_{3q} by q.

Expressions for pressure intensities are integrated over their respective domains to obtain the resultant pressure. The distance of the point of application of the resultant earth pressure is first obtained from the top of wall by integrating the moment of pressure intensity in each case and dividing it by the respective resultant earth pressure. The height of the point of application of the resultant earth pressure above the base of wall is obtained by subtracting this distance from the total height of the wall.

The resultant earth pressure and the height of its point of application

above the base of the wall in each case is expressed in nondimensional form as follows:

for case I:

$$K_\gamma = \frac{P_{1\gamma}}{\left(\frac{1}{2}\right)\gamma H^2} = \frac{\int_0^H p_{1\gamma}\, dy}{\left(\frac{1}{2}\right)\gamma H^2} \quad \ldots\ldots (28)$$

$$\frac{\bar{H}_\gamma}{H} = 1 - \frac{\int_0^H p_{1\gamma} \cdot y \cdot dy}{H \int_0^H p_{1\gamma}\, dy} \quad \ldots\ldots (29)$$

$$K_q = \frac{P_{1q}}{qH} = \frac{\int_0^H p_{1q}\, dy}{qH} \quad \ldots\ldots (30)$$

$$\frac{\bar{H}q}{H} = 1 - \frac{\int_0^H p_{1q} \cdot y \cdot dy}{H \int_0^H p_{1q}\, dy} \quad \ldots\ldots (31)$$

for case II:

$$K_\gamma = \frac{P_{2\gamma}}{\left(\frac{1}{2}\right)\gamma H^2} = \frac{\int_0^{Z_1} p_{2\gamma}\, dy + \int_{Z_1}^H p'_{2\gamma}\, dy}{\left(\frac{1}{2}\right)\gamma H^2} \quad \ldots\ldots (32)$$

$$\frac{\bar{H}_\gamma}{H} = 1 - \frac{\int_0^{Z_1} p_{2\gamma} y\, dy + \int_{Z_1}^H p'_{2\gamma} y\, dy}{H\left(\int_0^{Z_1} p_{2\gamma}\, dy + \int_{Z_1}^H p'_{2\gamma}\, dy\right)} \quad \ldots\ldots (33)$$

$$K_q = \frac{P_{2q}}{qH} = \frac{\int_0^{Z_1} p_{2q}\, dy + \int_{Z_1}^H p'_{2q}\, dy}{qH} \quad \ldots\ldots (34)$$

$$\frac{\bar{H}_q}{H} = 1 - \frac{\int_0^{Z_1} p_{2q} y\, dy + \int_{Z_1}^H p'_{2q} y\, dy}{H\left(\int_0^{Z_1} p_{2q}\, dy + \int_Z^H p'_{2q}\, dy\right)} \quad \ldots\ldots (35)$$

for case III:

$$K_\gamma = \frac{P_{3\gamma}}{\left(\frac{1}{2}\right)\gamma H^2} = \frac{\int_0^{z_2} p_{3\gamma}\,dy + \int_{z_2}^{z_3} p'_{3\gamma}\,dy + \int_{z_3}^{H} p''_{3\gamma}\,dy}{\left(\frac{1}{2}\right)\gamma H^2} \quad \ldots\ldots\ldots (36)$$

$$\frac{\bar{H}_\gamma}{H} = 1 - \frac{\int_0^{z_2} p_{3\gamma} y\,dy + \int_{z_2}^{z_3} p'_{3\gamma} y\,dy + \int_{z_3}^{H} p''_{3\gamma} y\,dy}{H\left(\int_0^{z_2} p_{3\gamma}\,dy + \int_{z_2}^{z_3} p'_{3\gamma}\,dy + \int_{z_3}^{H} p''_{3\gamma}\,dy\right)} \quad \ldots\ldots\ldots (37)$$

$$K_q = \frac{P_{3q}}{qH} = \frac{\int_0^{z_2} p_{3q}\,dy + \int_{z_2}^{z_3} p'_{3q}\,dy + \int_{z_3}^{H} p''_{3q}\,dy}{qH} \quad \ldots\ldots\ldots (38)$$

$$\frac{\bar{H}_q}{H} = 1 - \frac{\int_0^{z_2} p_{3q} y\,dy + \int_{z_2}^{z_3} p'_{3q} y\,dy + \int_{z_3}^{H} p''_{3q} y\,dy}{H\left(\int_0^{z_2} p_{3q}\,dy + \int_{z_2}^{z_3} p'_{3q}\,dy + \int_{z_3}^{H} p''_{3q}\,dy\right)} \quad \ldots\ldots\ldots (39)$$

It should be mentioned that the closed-form solutions of these equations have been obtained. The details of the derivations are available elsewhere (Garg 1988).

Parametric Analysis

Eqs. (28)–(39) were solved using the following ranges of the listed parameters: ϕ has a range of 30°–40°, at 5° intervals (where $\delta = 2/3\phi$); D_μ has a range of 0.2–2.0, at variable intervals; and L/H has a range of 0.0–1.0 of intervals of 0.2.

A typical plot of nondimensional pressure-intensity coefficients with the height of the wall is shown in Fig. 4. It is observed that the pressure intensity becomes negative somewhere along the height of the wall, depending upon the angle of internal friction ϕ of the soil and the amount of reinforcement (D_μ and L/H) in the fill. The resultant earth pressure is obtained by integrating the positive earth-pressure intensity diagram and then maximizing it with respect to the wedge angle θ. This leads to the critical wedge angle θ_{cr}. Resultant active earth-pressure coefficients and the corresponding points of application were obtained using θ_{cr} in (28)–(39). They are shown in Figs. 5–7.

It may be noted from Figs. 5–7 that the nondimensional coefficients, K_γ and K_q, diminish sharply with an increase in the L/H ratio up to around 0.6, and thereafter either become constant or decrease marginally depending on the values of D_μ and ϕ. Further, K_γ and K_q diminish with an increase in the spacing coefficient D_μ; this reduction in their values become insignificant when $D_\mu > 1.0$. The plots of $(\bar{H}_\gamma/H)$ and $(\bar{H}_q/H)$ [Figs. 5(*b*)–7(*b*)] show that the points of application of the resultant earth pressures shift sharply downward toward the base of wall for $L/H \geq 0.6$.

Model Tests

Verification of the analytical findings was attempted using model experiments on a 12-mm thick mild steel wall (L = 865 mm and H = 990 mm)

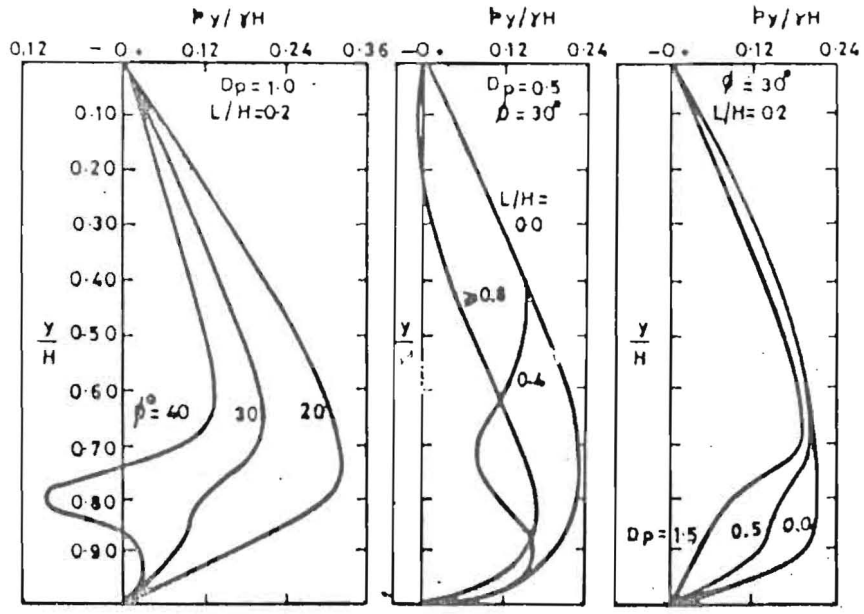

FIG. 4. Influence of ϕ, L/H, and Spacing Coefficient D_p on Pressure Distribution Pattern behind Wall

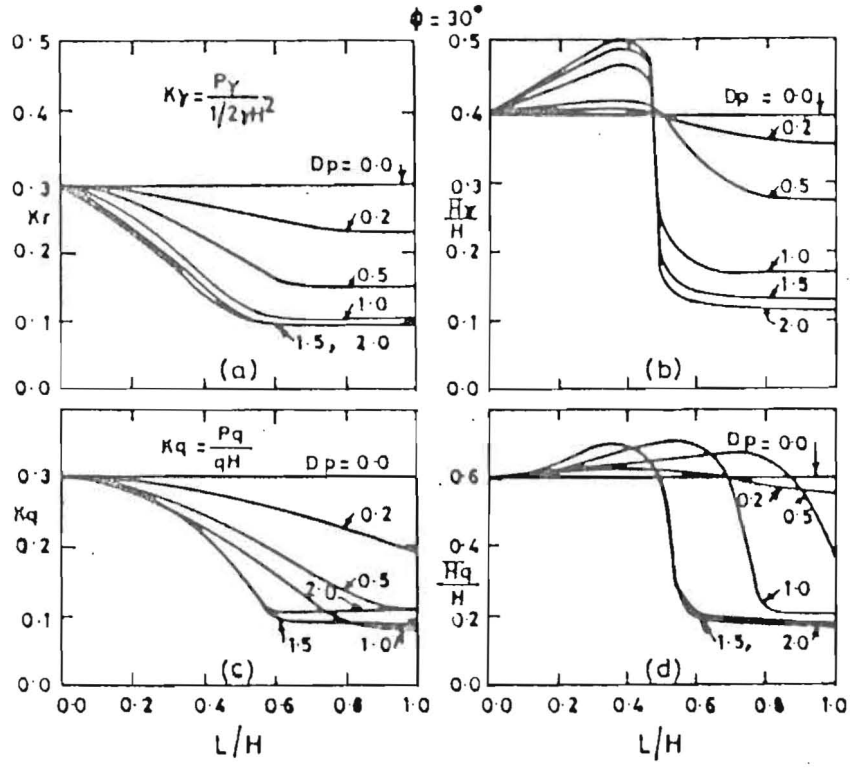

FIG. 5. Nondimensional Charts for Resultant Pressure and Height of Point of Application: (*a*) *a* and *b* Due to Backfill; (*b*) *c* and *d* Due to Surcharge Loading (ϕ = 30°)

in a tank with dimensions shown in Fig. 8. A locally available uniform sand (D_{10} = 0.09 mm, Unified Soil Classification System (USCS) group symbol = SP, e_{max} = 0.99, e_{min} = 0.535, D_R = 73%, γ = 16 kN/m^3, and ϕ = 39°) was used. Strips of aluminium (width = 4.00 cm, thickness = 0.03 cm) and bamboo (width = 2.2 cm, thickness = 0.103 cm) were used as reinforcement. The angles of sliding friction between the reinforcement and the

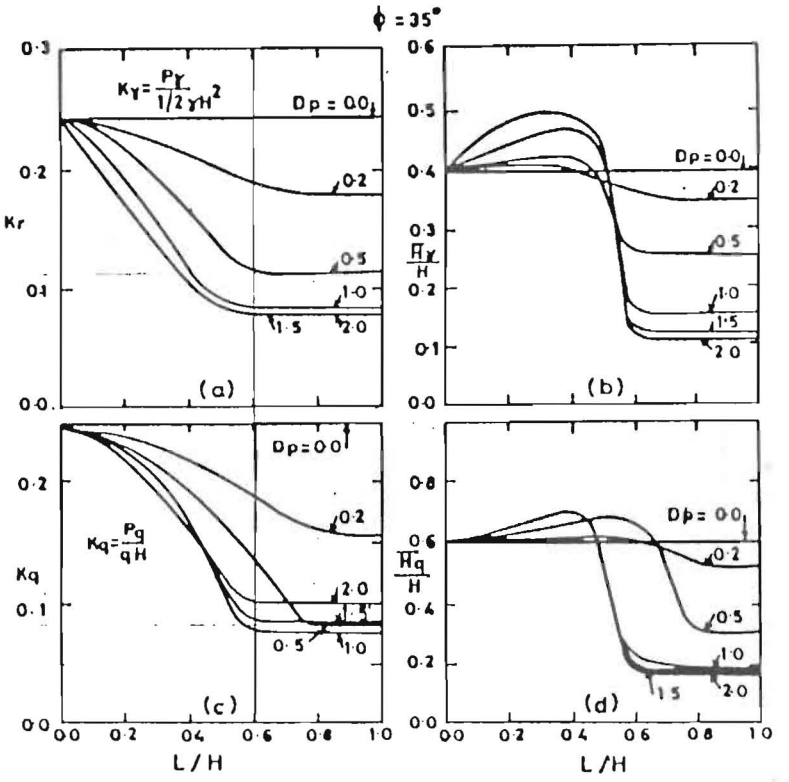

FIG. 6. Nondimensional Charts for Resultant Pressure and Height of Point of Application: (*a*) *a* and *b* Due to Backfill; (*b*) *c* and *d* Due to Surcharge Loading (ϕ = 35°)

sand determined from laboratory box shear tests were found to be 30° and 34°, respectively. The intensity of normal stress was varied from 0.25 kg/cm² to 2.0 kg/cm². A section of one side of the tank was constructed of a 12-mm thick glass sheet to allow observation of the rupture surface. The lower end of the wall was ground to a knife edge and was fixed to the tank base through hinges.

The lateral thrust on the wall was measured by a horizontally held calibrated proving ring attached to a screw jack at a height of 450 mm above the base of wall. The lateral displacement of the wall was recorded using dial gages at three different heights on the wall. The wall was initially clamped in a vertical position, and fill was placed by a rainfall technique to give an average dry density of 16.0 kN/m³ (D_R = 73%). The fill was placed in layers, and the top surface of each layer was leveled prior to the placement of reinforcing strips at the specified horizontal spacing. The strips were aligned perpendicularly to the wall, just touching its inner face. Surcharge loading was applied by cast-iron weights placed over a mild steel sheet that rested directly on the surface of the fill reinforced with aluminium strips. Tests with surcharge loading on the surface of the fill reinforced with bamboo strips could not be performed due to lack of time. The wall was unclamped after the full height of the backfill was attained and surcharge load was applied (if applicable). The thrust corresponding to these conditions was recorded. Subsequently, the wall was allowed to rotate gradually about its base by operating the screw jack. The force corresponding to each position of the wall was recorded as the rotation of the wall was continued beyond

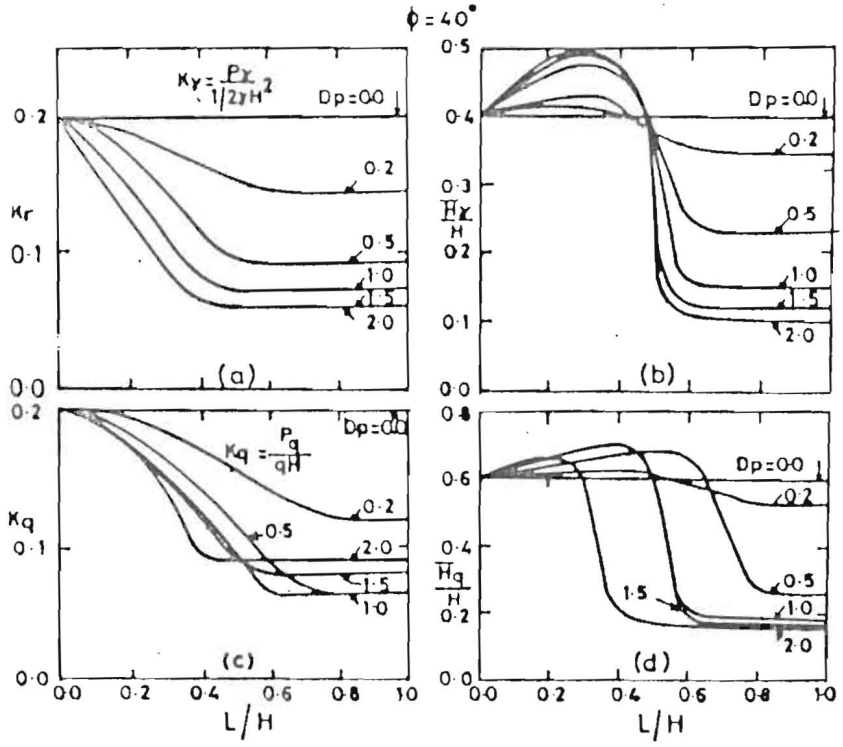

FIG. 7. Nondimensional Charts for Resultant Pressure and Height of Point of Application: (*a*) *a* and *b* Due to Backfill; (*b*) *c* and *d* Due to Surcharge Loading ($\phi = 40°$)

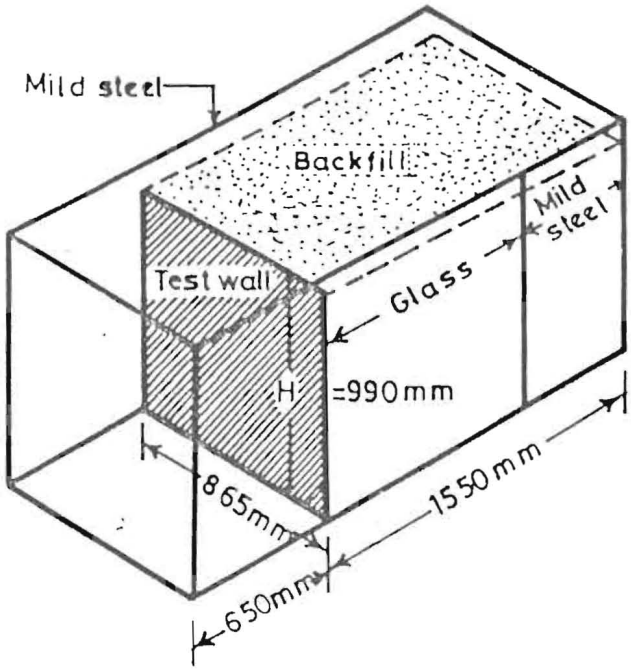

FIG. 8. Dimensional Sketch of Test Tank

that needed for the active state. The shape and size of the failure wedge in each test was observed by breaks in bands of colored sand through the glass plate.

Details of the tests performed on the model retaining wall in the laboratory are provided in Table 1. As evident from this table, the test conditions were varied to show the influences of D_p, the L/H ratio, and the surcharge

TABLE 1. Details of Model Tests

Test number (1)	Reinforcement (2)	Test Details				Intensity of surcharge loading (kN m^2) (7)
		D_r (3)	L/H (4)	S_1 (cm) (5)	S_2 (cm) (6)	
1	None	—[a]	—[a]	—[a]	—[a]	0
2	Bamboo	0.2	1.0	21	35	0
3	Bamboo	0.5	1.0	21	14	0
4	Bamboo	0.5	0.8	21	14	0
5	Bamboo	0.5	0.6	21	14	0
6	Bamboo	0.5	0.4	21	14	0
7	Bamboo	0.5	0.2	21	14	0
8	None	—[a]	—[a]	—[a]	[a]	10.0
9	Aluminium	0.2	1.0	22.00	52	0
10	Aluminium	0.5	1.0	21.75	21	0
11	Aluminium	0.5	1.0	21.75	21	10.0
12	Aluminium	0.5	0.6	21.75	21	10.0
13	Aluminium	0.5	0.4	21.75	21	10.0

[a]Unreinforced fill.

intensity q on the resulting lateral pressures. A typical set of results is shown in Fig. 9, and a summary of all the results is given in Tables 2 and 3. It may be noted that the results are presented in the form of moments, obtained by multiplying the observed lateral thrust by the moment arm of 450 mm (the height of the screw jack above the base of wall). Details of the test setup and procedure are given elsewhere (Garg 1988).

In the preliminary evaluations, the measured moments were found to be significantly lower (40%–50%) than their respective theoretical values. Thus, a method to correct for end effects was needed.

The height of the test wall (99 cm) was slightly more than its length (86.5 cm). A common observation in almost all the model experiments was that during the initial stages of the outward movement of the screw jack, which resulted in reduced earth pressure on the wall, the wall either did not move at all or moved insignificantly, confirming that the resisting frictional forces on the two sides of the test tank were at least partly responsible for the experimental values of the active earth pressure being lower than the theoretical ones. Side frictional force could be estimated by assuming an appropriate angle of wall friction for steel and for glass. The value for steel δ_1 was taken equal to $2/3\phi$, the same as for the test retaining wall, and that for glass δ_2 equal to $1/3\phi$.

The area on the two opposite sides of the tank that contributed to the resisting frictional force was assumed to be bounded by the triangular failure wedge in the active condition. Mathematical expressions derived to compute the frictional forces and their moments are as follows:

$$P_{F\gamma} = \frac{1}{6}\left[K_o \gamma H^3 \tan\theta(\tan\delta_1 + \tan\delta_2)\right] \quad \ldots\ldots (40)$$

$$M_{F\gamma} = \frac{1}{12}\left[K_o \gamma H^4 \tan\theta(\tan\delta_1 + \tan\delta_2)\right] \quad \ldots\ldots (41)$$

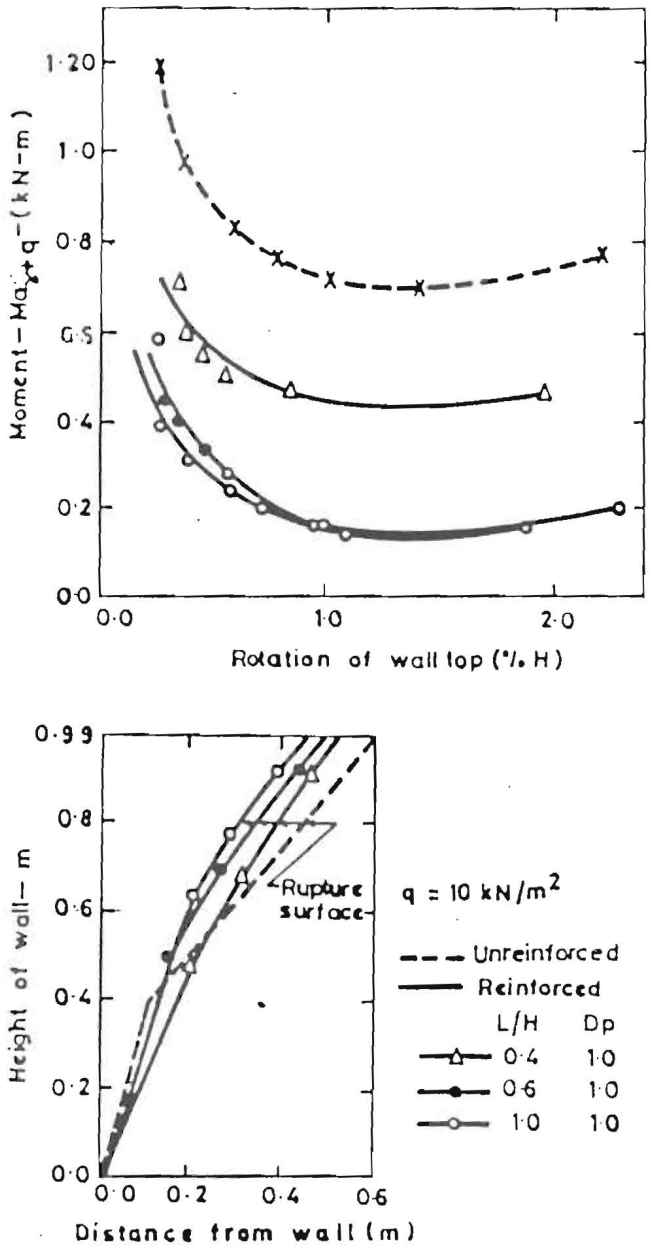

FIG. 9. Typical Results of Model Tests for Reinforced Backfill with Surcharge

$$P_{Fq} = \frac{1}{2}\left[K_o q H^2 \tan\theta(\tan\delta_1 + \tan\delta_2)\right] \quad \ldots\ldots\ldots\ldots\ldots\ldots\ldots\ldots (42)$$

$$M_{Fq} = \frac{1}{6}\left[K_o q H^3 \tan\theta(\tan\delta_1 + \tan\delta_2)\right] \quad \ldots\ldots\ldots\ldots\ldots\ldots\ldots\ldots (43)$$

where $P_{F\gamma}$ and P_{Fq} = side frictional forces due to backfill and surcharge load, respectively; $M_{F\gamma}$ and M_{Fq} = moments about base of the side frictional forces $P_{F\gamma}$ and P_{Fq}, respectively; $K_o = (1 - \sin\phi)$; $\delta_1 = 2/3\phi$ = angle of wall friction between the sand and the mild steel; and $\delta_2 = 1/3\phi$ = angle of wall friction between the sand and the glass plate.

The experimental and the net theoretical moments (net theoretical moment = total theoretical moment − total frictional moment on the two

TABLE 2. Summary of Model Test Results Using Aluminium Strips as Reinforcement

Test number (1)	Reinforcing Details		Surcharge, q (kN m^2) (4)	Measured force (kN) (5)	Rotation of wall top (%H) (6)	Angle of rupture plane, θ (deg) (7)	Moment (kN-m) (8)
	D_r (2)	L/H (3)					
1	—	—	—	0.62	1.50	23	0.28
9	0.2	1.0	—	0.31	1.24	20	0.14
10	0.5	1.0	—	0.17	1.25	14	0.08
8	—	—	10	1.64	1.36	31	0.74
11	0.5	1.0	10	0.32	1.20	24	0.15
12	0.5	0.6	10	0.29	1.30	26	0.13
13	0.5	0.4	10	1.00	1.34	27	0.45

TABLE 3. Summary of Model Test Results Using Bamboo Strips as Reinforcement

Test number (1)	Reinforcing Details		Measured force (kN) (4)	Rotation of wall top (%H) (5)	Angle of rupture plane, θ (deg) (6)	Moment (kN-m) (7)
	D_r (2)	L/H (3)				
2	0.2	1.0	0.33	1.30	18	0.15
3	0.5	1.0	0.14	1.25	13	0.06
4	0.5	0.8	0.18	1.25	13	0.06
5	0.5	0.6	0.14	1.28	14	0.07
6	0.5	0.4	0.32	1.40	23	0.15
7	0.5	0.2	0.60	1.45	23	0.27

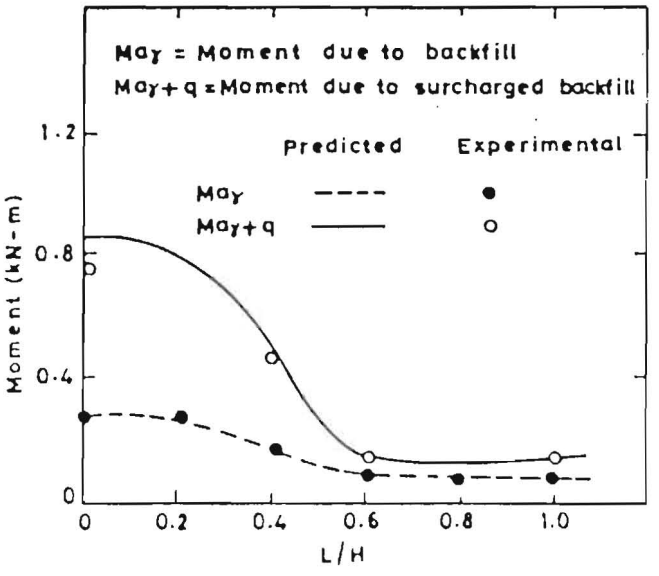

FIG. 10. Comparison of Analytical and Experimental Results

well (Fig. 10), suggesting that the proposed analytical approach is valid for designing rigid walls with reinforced fill that supports surcharge loading on its surface.

Guidelines for Practical Application

The following steps may be adopted for designing a retaining wall using the proposed theory:

1. Collect the data for which the wall is to be designed: the height of the wall H, and the density γ and the angle of internal friction ϕ of the fill material; the coefficient of base friction μ; the allowable soil pressure q_a, and the intensity of the surcharge load on the fill q.
2. Select the reinforcing material and obtain its frictional characteristics f^* and permissible tensile stress σ_t.
3. Assume suitable values of L/H and D_p. For economical design, it is recommended to adopt $L/H = 0.6$, and D_p between 0.5 and 1.0.
4. Using Figs. 5, 6, or 7, obtain K_γ, $\bar{H}_\gamma/H$, K_q, and $\bar{H}_q/H$ for the appropriate value of ϕ, and the assumed values of L/H and D_p.
5. Select suitable reinforcing strip dimensions, b and w. The horizontal and vertical spacings of the reinforcing strips, i.e., S_x and S_z, may be kept equal. Note that

$$S_x S_z = \frac{f^* w H}{D_p} \qquad (44)$$

By solving (44) for given values of f^* and H and assumed values of D_p and w, values for S_x and S_z are obtained.

6. The tension in the bottommost strip T_B will be the maximum and is given by

$$T_B = [\gamma H(K_{\gamma o} - K_\gamma) + q(K_{qo} - K_q)] S_x \cdot S_z \qquad (45)$$

where $K_{\gamma o}$ and K_{qo} are earth-pressure coefficients for unreinforced backfill obtained from Figs. 5, 6, or 7 for $L/H = 0.0$. For safe design, $T_B \leq$ the allowable tensile strength of the reinforcing strip, i.e., $T_B \leq \sigma_t \cdot b \cdot w$.

7. The section of the wall is then checked for sliding, overturning, and bearing failure using the resultant earth-pressure values $P_\gamma(\gamma H^2 K_\gamma/2)$ and $P_q(qHKq)$, and their corresponding points of application defined by $\bar{H}_\gamma$ and $\bar{H}_q$.

It may be noted that the proposed method is also applicable for mat-type reinforcement, i.e., using geotextile or geogrid. In the case of mat-type reinforcement

$$D_p = \frac{f^* H}{S_z} \qquad (46)$$

and

$$T_B = [\gamma H(K_{\gamma o} - K_\gamma) + q(K_{qo} - K_q)] \cdot S_z \qquad (47)$$

Therefore, values of S_z may be obtained directly by comparing T_B with the tensile strength of the geotextile or geogrid. Usually in this case, the value

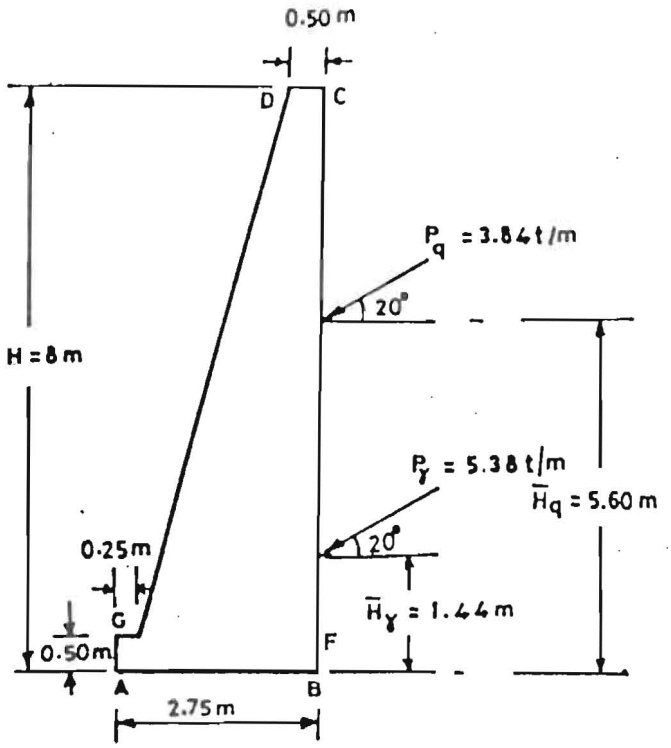

FIG. 11. Trial Section of Retaining Wall Selected for Design

of D_p will be more than 2.0. Values of earth-pressure coefficients (Figs. 5–7) may be obtained using the curves corresponding to $D_p = 2.0$, since values of D_p higher than 2.0 do not significantly affect the earth-pressure coefficients.

Design Example

1. Take the following data as given: $H = 8$ m, $\gamma = 1.6t/m^3$, $\phi = 30°$, $\mu = 0.5$, $q_a = 30t/m^2$, and $q = 3t/m^2$. These are galvanized iron (GI) strips with $f^* = 0.75$ and $\sigma_t = 14{,}000t/m^2$.

2. Assume $L/H = 0.6$ ($L = 4.8$ m), and $D_p = 1.0$, from Fig. 5.

3. For $\phi = 30°$, $D_p = 1.0$ and $L/H = 0.6$, $K_\gamma = 0.105$, $K_{\gamma o} = 0.30$, $(\bar{H}_\gamma/H) = 0.18$, $\bar{H}_\gamma = 1.44$ m, $K_q = 0.16$, $K_{qo} = 0.30$, $(\bar{H}_q/H) = 0.71$, and $\bar{H}_q = 5.6$ m.

4. Selecting 3-mm thick and 100-mm wide reinforcing strips of galvanized iron and taking $S_x = S_z$

$$D_p = 1.0 = \frac{f^* w H}{S_x S_z} = \frac{0.75 \times 0.10 \times 8.0}{S_z^2} \quad \ldots\ldots\ldots\ldots\ldots\ldots\ldots\ldots (48)$$

and $S_z = 0.775$ m. Adopt $S_x = S_z = 0.75$ m.

5. $$T_B = [\gamma H(K_{\gamma o} - K_\gamma) + q(K_{qo} - K_q)]S_x \cdot S_z \quad \ldots\ldots\ldots\ldots\ldots\ldots (49a)$$

and

$$T_B = [1.6 \times 8(0.3 - 0.105) + 3(0.3 - 0.16)]0.75 \times 0.75 = 1.64t \quad \ldots\ldots (49b)$$

The allowable tensile strength = $14{,}000 \times 0.10 \times 0.003 = 4.2t$. Since $T_B < 4.2t$, it is therefore safe.

6. A trial wall section as shown in Fig. 11 was chosen for checking its stability for pressures: $P_\gamma = (1/2)\gamma H^2 \cdot K_\gamma = (1/2) \times 1.6 \times 8^2 \times 0.105 = 5.38t/\text{m}$, acting at 1.44 m from the base; and $P_q = q \cdot H \cdot K_q = 3 \times 8 \times 0.16 = 3.84$, acting at 5.6 m from the base.

By checking the stability of the wall in the conventional way, we obtained a factor of safety against sliding = 1.51, a factor of safety against overturning = 2.2, and a maximum base pressure = $15t/\text{m}^2$.

Conclusions

The following major conclusions have been determined from this study:

1. Unattached reinforcing strips, embedded in the cohesionless backfill behind a rigid retaining wall, are effective in reducing the lateral earth pressure on the wall.
2. The extent of reduction in the resultant pressure will depend on the amount of reinforcement present in the backfill. Pressures due to both backfill and surcharge loading are reduced about 50% for all practical values of the spacing coefficient D_p.
3. Although the point of application of the resultant of lateral earth pressures (due to both fill and surcharge loading) moves above the one-third height of the wall only for certain combinations of values of ϕ, D_p, and L/H, the overturning moment is less than the moment from pressure due to unreinforced fill.
4. The optimum length of reinforcing strips is found to be around 0.6 times the height of wall for most practical cases.
5. The results of model tests show the credibility of the analytical approach.
6. While the assumption of a coefficient of soil-reinforcement interface friction f^* independent of the influence of the height of overburden and the length of the reinforcing strip is in accord with the experimental data, further investigation is needed to establish a simple procedure for evaluating f^*

Appendix I. References

Garg, K. G. (1988). "Earth pressure behind retaining wall with reinforced backfill," thesis presented to the University of Roorkee, at Roorkee, India, in partial fulfillment of the requirements for the degree of Doctor of Philosophy.

Hausmann, M. R., and Lee, K. L. (1978). "Rigid model wall with soil reinforcement." *Proc., Symp. on Earth Reinforcement*, ASCE, 400–427.

Talwar, D. V. (1981). "Behaviour of reinforced earth in retaining structures and shallow foundations," thesis presented to the University of Roorkee, at Roorkee, India, in partial fulfillment of the requirements for the degree of Doctor of Philosophy.

APPENDIX II. NOTATION

The following symbols are used in this paper:

b = thickness of reinforcing element;
C_u = uniformity coefficient;
C_1, C_2, C_3 = constants depending upon ϕ, θ, and δ;
C_4 = KC_3;
D_p = spacing coefficient;
D_R = relative density;
f^* = coefficient of apparent soil-reinforcement friction;
H = height of wall;
H_q = height of point of application of earth pressure due to surcharge load above base;
H_γ = height of point of application of earth pressure due to backfill above base;
K = $2wf^*\gamma \tan \theta / S_x S_z$;
K_a = coefficient of active earth pressure;
K_o = coefficient of earth pressure at rest;
K_q = coefficient of active earth pressure for surcharge loading in case of reinforced backfill;
K_{qo} = coefficient of active earth pressure for surcharge loading in case of unreinforced backfill;
K_γ = coefficient of active earth pressure for reinforced backfill;
$K_{\gamma o}$ = coefficient of active earth pressure for unreinforced backfill;
L = total length of reinforcing strip;
l' = effective length of reinforcing strip;
M_{Fq} = moment due to the side frictional force P_{Fq}, on tank side, about base;
$M_{F\gamma}$ = moment due to side frictional force $P_{F\gamma}$, on tank side, about base;
M_q = moment of pressure due to surcharge load in active condition about base;
M_γ = moment due to backfill pressure in active condition about base;
$M_{\gamma-q}$ = moment of pressue due to backfill plus surcharge load in active condition about base;
P_{Fq} = frictional force on tank sides adjoining wall due to surcharge loading;
$P_{F\gamma}$ = frictional force on tank sides adjoining wall due to backfill;
P_1, P_2, P_3 = resultant active earth pressure;
P_{1q}, P_{2q}, P_{3q} = resultant active earth pressure due to surcharge loading;
$P_{1\gamma}, P_{2\gamma}, P_{3\gamma}$ = resultant active earth pressure due to backfill;
p = $p_\gamma + p_q$;

p_v = pressure acting on element of soil in vertical direction;

p_H = intensity of reaction on failure surface;

$p_1, p_2, p'_2, p_3, p'_3, p''_3$ = lateral earth pressure intensity on wall;

$p_{1q}, p_{2q}, p'_{2q}, p_{3q}, p'_{3q}, p''_{3q}$ = lateral earth pressure intensity on wall due to surcharge loading;

$p_{1\gamma}, p_{2\gamma}, p'_{2\gamma}, P_{3\gamma}, p'_{3\gamma}, p''_{3\gamma}$ = lateral earth pressure intensity on wall due to backfill;

q = intensity of surcharge loading;

q_a = allowable soil pressure;

S_x = horizontal spacing of reinforcement;

S_z = vertical spacing of reinforcement;

T_B = total tension in bottommost strip;

t = uniformly distributed tensile stress;

W = weight of slice or element of soil;

w = width of reinforcing strip;

y = distance along wall from top;

Z, Z_1, Z_2, Z_3 = depth from top;

γ = unit weight;

δ = angle of sliding friction/angle of wall friction;

δ_1 = angle of wall friction between steel and sand;

δ_2 = angle of wall friction between glass and sand;

θ = wedge angle with vertical;

θ_{cr} = critical wedge angle with vertical;

μ = coefficient of friction;

σ_t = permissible tensile stress in reinforcing strip;

σ_z = vertical stress in soil; and

ϕ = angle of internal friction of soil.